

1 Revision 2

2  
3 **Carbonic Acid Monohydrate**

4  
5 Evan H. Abramson<sup>1</sup>, Olivier Bollengier<sup>1</sup>, J. Michael Brown<sup>1</sup>, Baptiste Journaux<sup>1</sup>, Werner  
6 Kaminsky<sup>2</sup>, Anna Pakhomova<sup>3</sup>

7 <sup>1</sup> Department of Earth and Space Sciences, University of Washington, Seattle, Washington,  
8 98195, USA

9 <sup>2</sup> Department of Chemistry, University of Washington, Seattle, Washington, 98195, USA

10 <sup>3</sup> Deutsches Elektronen-Synchrotron, Hamburg, 22607, Germany

11  
12 **Abstract**

13 In the water-carbon dioxide system, above a pressure of 4.4 GPa, a crystalline phase consisting  
14 of an adduct of the two substances can be observed to exist in equilibrium with the aqueous fluid.  
15 The phase had been found to be triclinic, and its unit cell parameters determined, but the full  
16 crystalline, and even molecular, structure remained undetermined. Here, we report new diamond-  
17 anvil cell, x-ray diffraction data of a quality sufficient to allow us to propose a full structure. The  
18 crystal exists in the  $P\bar{1}$  space group. Unit cell parameters (at 6.5 GPa and 140°C) are  
19  $a = 5.8508(14)$  Å,  $b = 6.557(5)$  Å,  $c = 6.9513(6)$  Å,  $\alpha = 88.59(2)^\circ$ ,  $\beta = 79.597(13)^\circ$ , and  
20  $\gamma = 67.69(4)^\circ$ . Direct solution for the heavy atoms (carbon and oxygen) revealed CO<sub>3</sub> units, with  
21 co-planar, but isolated, O units. Construction of a hydrogen network, in accordance with the  
22 requirements of hydrogen bonding and with minimum allowed distances between non-bonded

23 atoms, indicates that the phase consists of a monohydrate of carbonic acid ( $\text{H}_2\text{CO}_3 \cdot \text{H}_2\text{O}$ ) with the  
24 carbonic acid molecule in the cis-trans configuration. This is the first experimental determination  
25 of the crystalline structure of a  $\text{H}_2\text{CO}_3$  compound. The structure serves as a guide for ab initio  
26 calculations that have until now explored only anhydrous  $\text{H}_2\text{CO}_3$  solids, while validating  
27 calculations that indicated that high pressures should stabilize  $\text{H}_2\text{CO}_3$  in the solid state. If 4.4  
28 GPa is the lowest pressure at which the phase is thermodynamically stable, this probably  
29 precludes its existence in our solar system, although it may exist on larger, volatile-rich  
30 exoplanets. If, however, its range of stability extends to lower pressures at lower temperatures  
31 (which possibility has not yet been adequately explored) then it might have been be a stable form  
32 of  $\text{CO}_2$  within the water-rich moons and dwarf planets prior to differentiation, and might still  
33 exist on an undifferentiated Callisto.

34

35 Keywords: carbonic acid,  $\text{CO}_2$ , hydrate, high-pressure, single-crystal X-ray diffraction,  
36 exoplanets

37

38

39

## Introduction

40 Water and carbon dioxide are ubiquitous compounds in the biological and geological sciences.  
41 Their 1:1 adduct, carbonic acid ( $\text{H}_2\text{CO}_3$ ), and its two anions, bicarbonate ( $\text{HCO}_3^-$ ) and carbonate  
42 ( $\text{CO}_3^{2-}$ ), engage in an important set of reactions governing the solubility of  $\text{CO}_2$  and the pH of  
43 systems critical to life and planetary processes. However, owing to unfavorable kinetics and  
44 equilibrium constants at ambient conditions (Loerting et al. 2000), molecular carbonic acid has

45 long eluded detailed experimental observation and, as described below, a crystalline structure  
46 had not previously been determined. Recently, Wang et al. (2016) claimed to have observed the  
47 formation of solid carbonic acid at high pressures, and Abramson et al. (2017) demonstrated that  
48 the observed phase can exist in thermodynamic equilibrium with the aqueous fluid for pressures  
49 beyond a quadruple point at 4.4 GPa. Preliminary X-ray results indicated that the new phase was  
50 triclinic, but their quality did not allow a refinement of the crystal structure. Here, new X-ray  
51 diffraction data of the high-pressure phase provide further insight into its structure. Despite  
52 remaining uncertainties pertaining to the hydrogen network, the results confirm the presence of  
53 H<sub>2</sub>CO<sub>3</sub> molecules, and indicate that the crystal consists of a monohydrate of the acid. Our results  
54 complete the initial experimental reports describing that phase, validate calculations which  
55 indicated that high pressures should stabilize H<sub>2</sub>CO<sub>3</sub> in the solid state, and offer a structure for a  
56 H<sub>2</sub>CO<sub>3</sub> hydrate as a guide to further calculations.

57

58

### Prior Studies

59 Over the past three decades, attempts to synthesize H<sub>2</sub>CO<sub>3</sub> have led to the development of  
60 numerous protocols divided among four main strategies. 1. **The vacuum thermolysis of**  
61 **carbonates** led to the first reported synthesis of H<sub>2</sub>CO<sub>3</sub>, in the vapor phase; originally using  
62 ammonium bicarbonate (Terlouw et al. 1987), the process was more recently accomplished with  
63 di-tert-butyl carbonate (Reisenauer et al. 2014). 2. **The irradiation of CO<sub>2</sub> and H<sub>2</sub>O ices**  
64 produced the first H<sub>2</sub>CO<sub>3</sub> solid; the initial experiment involved the proton irradiation of CO<sub>2</sub> +  
65 H<sub>2</sub>O mixtures (Moore and Khanna 1991), but both UV photolysis (Gerakines et al. 2000; Wu et  
66 al. 2003) and electron irradiation of the mixtures (Zheng and Kaiser 2007), as well as the proton

67 irradiation of pure CO<sub>2</sub> ice (Brucato et al. 1997; Garozzo et al. 2008) have also been successful.  
68 **3. The ionization of CO<sub>2</sub> and H<sub>2</sub>O gases** has been used to produce radicals for recombination  
69 into H<sub>2</sub>CO<sub>3</sub>, either directly in the gas phase (Mori et al. 2009, 2011), or in the solid state by  
70 deposition of OH radicals onto CO ice (Oba et al. 2010). 4. Finally, **the protonation of**  
71 **carbonates** has been explored to produce H<sub>2</sub>CO<sub>3</sub> in various states; short-lived aqueous H<sub>2</sub>CO<sub>3</sub>  
72 was produced by reacting acids with NaHCO<sub>3</sub> (Falcke and Eberle 1990; Lam et al. 2014),  
73 Na<sub>2</sub>CO<sub>3</sub> (Soli and Byrne 2002), or DCO<sub>3</sub><sup>-</sup> (Adamczyk et al. 2009); similarly, solid H<sub>2</sub>CO<sub>3</sub> has  
74 been synthesized through reactions in aqueous glasses, combining acids with K<sub>2</sub>CO<sub>3</sub> or KHCO<sub>3</sub>  
75 (Hage et al. 1995, 1996; Bernard et al. 2013), or particulate CaCO<sub>3</sub> (Bernard et al. 2012); as well,  
76 dry vapors of acids reacted with particulate CaCO<sub>3</sub> (Al-Hosney and Grassian 2004, 2005; Al-  
77 Hosney et al. 2005) have produced adsorbed H<sub>2</sub>CO<sub>3</sub>.

78  
79 Following the first synthesis of solid H<sub>2</sub>CO<sub>3</sub> (Moore and Khanna 1991), spectral analyses have  
80 typically relied upon IR absorption and/or Raman spectroscopies. Direct confirmation of the  
81 molecular composition has been confined to the gas phase syntheses, through neutralization-  
82 reionization mass spectrometry (Terlouw et al. 1987) and microwave spectroscopy (Mori et al.  
83 2009, 2011); X-ray diffraction patterns were reported for an amorphous solid (Winkel et al.  
84 2007), however attempts to provide diffraction patterns of a crystallized sample were  
85 inconclusive (Mitterdorfer et al. 2012; Bernard et al. 2013). These limitations gave room to the  
86 belief, for two decades, that two different configurations of H<sub>2</sub>CO<sub>3</sub> (then designated as α-H<sub>2</sub>CO<sub>3</sub>  
87 and β-H<sub>2</sub>CO<sub>3</sub>) had their own distinct amorphous, crystalline, and vapor phases preserved through  
88 sublimation and condensation (Hage et al. 1995, 1996, 1998; Bernard et al. 2011, 2013); not until

89 2014 was it discovered that only one of these phases ( $\beta$ -H<sub>2</sub>CO<sub>3</sub>) pertained to H<sub>2</sub>CO<sub>3</sub>, while the  
90 putative  $\alpha$ -H<sub>2</sub>CO<sub>3</sub> actually consisted of the related monomethyl ester (Reisenauer et al. 2014).

91

92 Efforts to predict possible crystalline structure(s) for H<sub>2</sub>CO<sub>3</sub> through ab initio calculations have  
93 yielded a variety of solutions with differences in energy levels smaller than the uncertainties  
94 (Winkel et al. 2007; Reddy et al. 2011). Simulations of the C-H-O system suggest that pressure  
95 has a stabilizing effect on H<sub>2</sub>CO<sub>3</sub>, allowing several of its polymorphs, and a polymerized form, to  
96 exist (at 0 K) between ~1 and ~300 GPa (Saleh and Oganov 2016). In contrast to the  
97 computational results, experimental studies of the H<sub>2</sub>O-CO<sub>2</sub> system under pressure had found  
98 only two gas hydrates of CO<sub>2</sub> (Sloan and Koh 2007; Tulk et al. 2014; Amos et al. 2017), both  
99 existing only below 1 GPa and decomposing into ices of their component molecules when  
100 brought to higher pressures (Hirai et al. 2010; Bollengier et al. 2013; Tulk et al. 2014; Massani et  
101 al. 2017). (The cryogenically prepared, amorphous carbonic acid, or its annealed form (Kohl et  
102 al. 2009), may be stable at high pressures but, to our knowledge, this possibility has not been  
103 tested. )

104

105 Recently, a new CO<sub>2</sub>-H<sub>2</sub>O compound was observed above 2.4 GPa and asserted to be H<sub>2</sub>CO<sub>3</sub>  
106 based on IR and Raman lines similar to those of the low pressure H<sub>2</sub>CO<sub>3</sub> solid (Wang et al.  
107 2016). Following this initial report, we (Abramson et al. 2017) demonstrated that this new phase  
108 can exist in equilibrium with an aqueous fluid (starting from a quadruple point with ices  
109 H<sub>2</sub>O(VII) and CO<sub>2</sub>(I), at 4.4 GPa and 165 °C), which allowed the growth of single crystals for  
110 purposes of X-ray diffraction. However, non-hydrostatic strains in the crystal degraded the

111 quality of the data, and only the lattice parameters of the triclinic crystal were determined; its full  
112 structure, and chemical composition, remained unknown.

113

114

### Methodology

115 A CO<sub>2</sub>-H<sub>2</sub>O mixture was loaded at the University of Washington into a Merrill-Bassett type  
116 diamond-anvil cell (DAC) equipped with a 40 μm thick rhenium gasket. The cell contents were  
117 estimated at 30 mol% CO<sub>2</sub> from visual observation of the loaded sample. Pressure was measured  
118 to a precision of 0.1 GPa, using the Raman scattering from a chip of cubic boron nitride (cBN)  
119 placed inside the sample chamber; excitation was provided by a 20 mW, 488 nm laser source.  
120 Temperature was measured to an accuracy of 1 K through use of type K thermocouples. Further  
121 details are given in Abramson et al. (2017). Single crystals were grown between pressures of 5  
122 and 6 GPa by slow cooling (2 °C/min) of the H<sub>2</sub>O-CO<sub>2</sub> fluid mixture after a few nuclei had been  
123 isolated (figure 1); after crystallization, further cooling brought the pressure to 6.5 GPa.

124

125 The DAC was brought to the European Synchrotron Radiation Facility in Grenoble, France, for  
126 single-crystal X-ray diffraction on beamline ID15b. Prior to data collection, the DAC was placed  
127 in an external resistive heating system and brought to 140 ±2 °C to allow partial annealing of  
128 residual strains; this produced an appreciable improvement in the sharpness of reflections. Data  
129 were acquired using a wavelength of 0.4108 Å and a beam diameter of 10 μm FWHM. The  
130 Bragg peaks from one crystal were collected on a MarCCD® flat panel detector (MAR555)  
131 using the scan mode from -28° to +28° with an increment of 0.5° and an exposure time of 1 s.  
132 The location of the collection spot (indicated in figure 1B) was chosen to provide a maximum

133 thickness of single crystal, to avoid areas suspected to be subject to a greater non-hydrostatic  
134 strain, and to limit shadowing from the gasket.

135

136 Data collection was 20.4% complete to  $25^\circ$  in  $\theta$ . In total, 243 reflections were collected, covering  
137 the indices  $-6 \leq h \leq 6$ ,  $-3 \leq k \leq 4$ , and  $-7 \leq l \leq 7$ . Of these, 165 reflections were symmetry  
138 independent with  $R_{\text{int}} = 0.0337$ . Indexing and unit cell refinement indicated a primitive triclinic  
139 lattice. The space group was found to be  $P \bar{1}$  (no. 2). The unit cell parameters closely match  
140 those previously obtained at the Advanced Light Source in Berkeley (Abramson et al. 2017).  
141 Angles ( $\alpha = 88.59(2)^\circ$ ,  $\beta = 79.60(1)^\circ$ , and  $\gamma = 67.69(4)^\circ$ ) agree within 0.1% while the new cell  
142 dimensions ( $a = 5.851(1) \text{ \AA}$ ,  $b = 6.557(5) \text{ \AA}$ , and  $c = 6.951(1) \text{ \AA}$ ) are 0.5% smaller, possibly due  
143 to a slight compression resulting from the elevated temperature of the DAC (pressure was not  
144 measured during data collection). The data were integrated and scaled using the CrysAlisPro  
145 software (Rigaku Oxford Diffraction, 2015). Empirical absorption corrections were applied using  
146 spherical harmonics, implemented in the SCALE3 ABSPACK scaling algorithm (Oxford  
147 Diffraction, 2006).

148

149

### Structure Refinement

150 A multi-step iterative approach based on plausible constraints was required to provide a full  
151 structure for this triclinic crystal. After an initial model was obtained by direct solution, the  
152 structure was completed by difference Fourier synthesis with SHELXL (Sheldrick 2015) using  
153 scattering factors from Waasmair and Kirfel (1995). All non-hydrogen atoms were refined  
154 anisotropically by full-matrix least-squares. The locations of hydrogen atoms were then

155 determined based on the geometry of the carbon-oxygen structures and appropriate hydrogen-  
156 bonding behavior. Crystallographic data are provided as supplementary material in a CIF file.  
157 The process used to refine the structure is detailed below.

158

159 Initially, the direct solution produced a partial model with two CO<sub>3</sub>-resembling electron density  
160 maxima per asymmetric unit of the space group. Two isolated oxygen atoms were found in the  
161 vicinity of the CO<sub>3</sub> groupings. The CO<sub>3</sub> and O components are co-planar but separated by more  
162 than 2 Å, precluding a covalent bond. To refine the CO<sub>3</sub> geometries, their angles and bond  
163 lengths were restrained to be as equivalent as possible while adequately fitting the data. In a  
164 search for a shorter C-O distance in each grouping (as expected from a double bond), only one  
165 out of nine possible permutations of one short and two long bonds per CO<sub>3</sub> gave a satisfying R1,  
166 and it was subsequently adopted. Since neither the bond lengths nor the angles were fixed, the  
167 existence of one double bond in, and the planarity of, each CO<sub>3</sub> was confirmed.

168

169 The last step in completing the structure consisted of placing hydrogen atoms in geometrically  
170 ideal positions. The relative orientations of the CO<sub>3</sub> were examined for possible H-bonds, for  
171 which distance and angles matter (figure 2). Starting with the single-bonded oxygens of the CO<sub>3</sub>,  
172 the closest receptor for the hydrogen of O4 is the double-bonded O3. O3 is also at an appropriate  
173 distance to act as a receptor for a hydrogen on O7. The geometries of the water molecules (O7  
174 and O8) were then restrained with hydrogens set at 0.8 Å, resulting in a quasi-rigid model  
175 allowed to rotate freely. The second hydrogen on O7 was assumed to bond with the closest out-  
176 of-plane oxygen acceptor. With O4 and O7 set with H-bonds to O3, the hydrogen on O5 was set



177 towards O8, giving the H<sub>2</sub>CO<sub>3</sub> molecule a cis-trans configuration. The hydrogen on O1 aligned  
178 appropriately for hydrogen bonding without an added constraint. Once this satisfactory network  
179 was complete, a few H···H distances fell in the 2.00-2.07 Å range, slightly below the minimum  
180 allowed distance of 2.1 Å, requiring an anti-bumping restraint. All hydrogens (with O-H bonds  
181 restrained at 0.8 Å) could finally be assigned an appropriate orientation.

182

183

### Discussion

184 The limited angular access available in a diamond-anvil cell, the low symmetry of the crystal,  
185 and the small scattering cross-section of the hydrogen atoms all contributed to the challenge of  
186 determining this structure. However, the direct method unambiguously determined the presence  
187 of the CO<sub>3</sub> and O components, yielding the formula with respect to C and O. The distances  
188 between neighboring components (CO<sub>3</sub> and O) imply that they are isolated, precluding the  
189 presence of more complex C-O-H molecules (notably the orthocarbonic acid H<sub>4</sub>CO<sub>4</sub> of  
190 equivalent bulk formula (Saleh and Oganov 2016), or dicarbonic acid H<sub>2</sub>C<sub>2</sub>O<sub>5</sub> (Zeller et al. 2005;  
191 Zhang et al. 2013)). Since only hydrogen atoms are available to bond with the CO<sub>3</sub>, molecular  
192 H<sub>2</sub>CO<sub>3</sub> is required in the structure. Consequently, the final crystal formula (CH<sub>4</sub>O<sub>4</sub>), the presence  
193 of carbonic acid and its ratio to water, and the co-planar arrangement within the same (110)  
194 planes of the oxygen and carbon of the carbonic acid, and oxygen of the water molecules, are  
195 definitive conclusions of this work, independent of the subsequent interpretative steps used to  
196 refine the hydrogen network. The final structure reached at the end of the last steps is fully  
197 compatible with our dataset. As well, the calculated density of 2.194 g/cm<sup>3</sup> exceeds that of

198 H<sub>2</sub>O(VII), 1.72 g/cm<sup>3</sup>, consistent with the observation that the monohydrate will sink in the same  
199 solution in which the latter will float (Abramson et al. 2017).

200

201 In our final structure, the H<sub>2</sub>CO<sub>3</sub> and H<sub>2</sub>O molecules are organized on parallel, H-bonded sheets  
202 in (110) lattice planes (figure 3). Within each sheet, H<sub>2</sub>CO<sub>3</sub> molecules form (hydrogen-bonded)  
203 chains parallel to the c-axis with water providing in-plane hydrogen bonding between adjacent  
204 chains. To our knowledge, ab initio calculations have only investigated pure H<sub>2</sub>CO<sub>3</sub> structures so  
205 far, limiting the relevance of direct comparisons with the present monohydrate; however, low-  
206 pressure structures have indeed been said to favor chain- or sheet-like configurations (with the  
207 planes of the individual H<sub>2</sub>CO<sub>3</sub> molecules coincident with the crystal planes) (Reddy et al. 2011;  
208 Saleh and Oganov 2016), as opposed to 3D networks for higher-pressure, polymerized structures  
209 (Saleh and Oganov 2016).

210

211 The main uncertainty in our solution is in the determination of the hydrogen network. The  
212 proximity of the H<sub>2</sub>CO<sub>3</sub> molecules suggests H bonds exist between them; in turn, the relative  
213 orientation of the molecules (i.e. the position of the C=O bonds) suggests that the H<sub>2</sub>CO<sub>3</sub> are in a  
214 cis-trans configuration (as explained in the Structure Refinement section). Although the cis-cis  
215 conformer has been identified as the most stable configuration for the isolated H<sub>2</sub>CO<sub>3</sub> molecule,  
216 for H-bonded H<sub>2</sub>CO<sub>3</sub> molecules, and for H<sub>2</sub>CO<sub>3</sub>-H<sub>2</sub>O complexes (see (Mori et al. 2009) and  
217 references therein, and (Bernard et al. 2013)), the cis-trans conformer is considered a close  
218 second (in comparison with the clearly less stable trans-trans), as well as a necessary step on the  
219 decomposition (formation) pathway to (from) CO<sub>2</sub> + H<sub>2</sub>O (Mori et al. 2009).

220

221

### Implications

222 The present work provides the first characterization of the structure of a crystal containing the  
223  $\text{H}_2\text{CO}_3$  molecule, which is additionally the only known example of a solid  $\text{H}_2\text{CO}_3$  compound in  
224 conditions of established thermodynamic equilibrium (i.e. a demonstrated, reversible transition).  
225 The results validate calculations that indicate that high pressures can stabilize  $\text{H}_2\text{CO}_3$  in the solid  
226 state (Saleh and Oganov, 2016). The confirmation of the existence of a stable  $\text{H}_2\text{CO}_3$  compound,  
227 of its formation in the hydrated state, and of equilibrium with the aqueous fluid, may prove  
228 useful both as a guide to future computational searches for stable structures within the  $\text{H}_2\text{O}-\text{CO}_2$   
229 system, and in stimulating further experimental exploration of this system.

230

231 In the absence of other  $\text{H}_2\text{O}-\text{CO}_2$  solids reported between 1.0 GPa (the upper limit of the known  
232  $\text{CO}_2$  gas hydrates) and 4.4 GPa (the lower end of the proven stability field of the present  
233 structure (Abramson et al. 2017)), the  $\text{H}_2\text{CO}_3$  monohydrate may define the lower pressure  
234 boundary of an extended domain of additional  $\text{H}_2\text{O}-\text{CO}_2$  compounds: the present monohydrate  
235 was reportedly observed up to 25 GPa (Wang et al. 2016), while simulations suggest a transition  
236 around  $\sim 300$  GPa from various polymorphs and polymers of  $\text{H}_2\text{CO}_3$  to  $\text{H}_4\text{CO}_4$  (Saleh and  
237 Oganov, 2016). Alternatively, this (or other) carbonic acid hydrate(s) may exist between 1 and  
238 4.4 GPa, but at temperatures below the solidus, where sluggish rates of solid-solid transitions  
239 would have precluded their observation (note that in common hydrate-forming systems, e.g.,  
240  $\text{H}_2\text{O}-\text{MgSO}_4$  (Chou and Seal 2007), lower temperatures favor the formation of higher hydrates).

241

242 Restricting our attention to the present  $\text{H}_2\text{CO}_3$  monohydrate, if 4.4 GPa is indeed the lower  
243 pressure limit of its thermodynamic stability, this would likely preclude its existence in our solar  
244 system. Ices within the (now differentiated) water-rich moons and dwarf planets of the outer  
245 solar system do not achieve sufficiently high pressures, while in Earth, Neptune and Uranus,  
246 temperatures at the requisite pressure are too high. Although radiolysis of mixed  $\text{H}_2\text{O}/\text{CO}_2$  ices,  
247 or proton implantation into water ice, is believed to produce  $\text{H}_2\text{CO}_3$  as a metastable molecule on  
248 the surfaces of icy bodies, there has been no evidence that the monohydrate is formed in these  
249 processes. If, however, lowering of temperature allows the hydrate to exist stably at lower  
250 pressures (and this hasn't yet been explored), then it might have been a stable form of  $\text{CO}_2$  within  
251 the water-rich moons and dwarf planets prior to differentiation, and might still exist on (a  
252 partially differentiated) Callisto. Of course, considering the prevalence of C-H-O fluids in  
253 planetary processes, the present  $\text{H}_2\text{CO}_3$  monohydrate may be supposed to exist in some of the  
254 (larger, volatile-rich) exoplanets of current interest.

255

256

### Acknowledgments

257 This work was partially funded by NASA Solar System Workings grant 80NSSC17K0775 and  
258 by the Icy Worlds node of NASA's Astrobiology Institute (08-NAI5-0021). Single-Crystal X-  
259 Ray diffraction data were acquired at the ID15B beamline of the European Synchrotron Research  
260 Facility, Grenoble, France. B. Journaux is being supported by the NASA Postdoctoral Program  
261 and the NASA Astrobiology Institute. The authors would like to thank S. Petitgirard, I. Collings  
262 and M. Hanfland for their scientific and technical support during the ID15b synchrotron beam  
263 time.

## References

264

265

266

267 Abramson, E.H., Bollengier, O., and Brown, J.M. (2017) Water-carbon dioxide solid phase  
268 equilibria at pressures above 4 GPa. *Scientific Reports*, 7, 821.

269

270 Adamczyk, K., Prémont-Schwarz M., Pines D., Pines E., and Nibbering E.T.J. (2009) Real-Time  
271 Observation of Carbonic Acid Formation in Aqueous Solution. *Science*, 326, 1690-1694.

272

273 Amos, D.M., Donnelly, M.-E., Teeratchanan, P., Bull, C.L., Falenty, A., Kuhs, W.F., Hermann,  
274 A., and Loveday, J.S. (2017) A Chiral Gas-Hydrate Structure Common to the Carbon  
275 Dioxide-Water and Hydrogen-Water Systems. *The Journal of Physical Chemistry Letters*, 8,  
276 4295-4299.

277

278 Al-Hosney, H.A., and Grassian, V.H. (2004) Carbonic Acid: An Important Intermediate in the  
279 Surface Chemistry of Calcium Carbonate. *Journal of the American Chemical Society*, 126,  
280 8068-8069.

281

282 Al-Hosney, H.A., and Grassian, V.H. (2005) Water, sulfur dioxide and nitric acid adsorption on  
283 calcium carbonate: A transmission and ATR-FTIR study. *Physical Chemistry Chemical  
284 Physics*, 7, 1266-1276.

285

286 Al-Hosney, H.A., Carlos-Cuellar, S., Baltrusaitis, J., and Grassian, V.H. (2005) Heterogeneous  
287 uptake and reactivity of formic acid on calcium carbonate particles: a Knudsen cell reactor,  
288 FTIR and SEM study. *Physical Chemistry Chemical Physics*, 7, 3587-3595.

289

290 Bernard, J., Seidl, M., Kohl, I., Liedl, K.R., Mayer, E., Gálvez, Ó., Grothe, H., and Loerting T.  
291 (2011) Spectroscopic Observation of Matrix-Isolated Carbonic Acid Trapped from the Gas  
292 Phase. *Angewandte Chemie International Edition*, 50, 1939-1943.

293

294 Bernard, J., Seidl, M., Mayer, E., and Loerting, T. (2012) Formation and Stability of Bulk  
295 Carbonic Acid (H<sub>2</sub>CO<sub>3</sub>) by Protonation of Tropospheric Calcite. *ChemPhysChem*, 13, 3087-  
296 3091.

297

298 Bernard, J., Huber, R.G., Liedl, K.R., Grothe, H., and Loerting, T. (2013) Matrix Isolation  
299 Studies of Carbonic Acid – The Vapor Phase above the β-Polymorph. *Journal of the*  
300 *American Chemical Society*, 135, 7732-7737.

301

302 Bollengier, O., Choukroun, M., Grasset, O., Le Menn, E., Bellino, G., Morizet, Y., Bezacier, L.,  
303 Oancea, A., Taffin, C., and Tobie G. (2013) Phase equilibria in the H<sub>2</sub>O-CO<sub>2</sub> system between  
304 250-330 K and 0-1.7 GPa: Stability of the CO<sub>2</sub> hydrates and the H<sub>2</sub>O-ice VI at CO<sub>2</sub>  
305 saturation. *Geochimica et Cosmochimica Acta*, 119, 332-339.

306

- 307 Brucato, J.R., Palumbo, M.E., and Strazzulla G. (1997) Carbonic Acid by Ion Implantation in  
308 Water/Carbon Dioxide Ice Mixtures. *Icarus*, 125, 135-144.  
309
- 310 Chou, I-M., and Seal, R.R. II (2007) Magnesium and calcium sulfate stabilities and the water  
311 budget of Mars. *Journal of Geophysical Research: Planets*, 112, E11004.  
312
- 313 Falcke, H., and Eberle, S.H. (1990) Raman spectroscopic identification of carbonic acid. *Water*  
314 *Research*, 24, 685-688.  
315
- 316 Garozzo, M., Fulvio, D., Gomis, O., Palumbo, M.E., and Strazzulla, G. (2008) H-implantation in  
317 SO<sub>2</sub> and CO<sub>2</sub> ices. *Planetary and Space Science*, 56, 1300-1308.  
318
- 319 Gerakines, P.A., Moore, M.H., and Hudson, R.L. (2000) Carbonic acid production in H<sub>2</sub>O:CO<sub>2</sub>  
320 ices. UV photolysis vs. proton bombardment. *Astronomy and Astrophysics*, 357, 793-800.  
321
- 322 Hage, W., Hallbrucker, A., and Mayer, E. (1995) A Polymorph of Carbonic Acid and its Possible  
323 Astrophysical Relevance. *Journal of the Chemical Society, Faraday Transactions*, 91, 2823-  
324 2826.  
325
- 326 Hage, W., Hallbrucker, A., and Mayer, E. (1996) Metastable intermediates from glassy solutions.  
327 Part 4. FTIR spectra of β-carbonic acid and its <sup>2</sup>H and <sup>13</sup>C isotopic forms, isolated from  
328 aqueous solution. *Journal of the Chemical Society, Faraday Transactions*, 92, 3197-3209.

329

330 Hage, W., Liedl, K.R., Hallbrucker, A., and Mayer, E. (1998) Carbonic Acid in the Gas Phase  
331 and Its Astrophysical Relevance. *Science*, 279, 1332-1335.

332

333 Hirai, H., Komatsu, K., Honda, M., Kawamura, T., Yamamoto, Y., and Yagi, T. (2010) Phase  
334 changes of CO<sub>2</sub> hydrate under high pressure and low temperature. *The Journal of Chemical*  
335 *Physics*, 133, 124511.

336

337 Kohl, I., Winkel, K., Bauer, M., Liedl, K.R., Loerting, T., and Mayer, E. (2009) Raman  
338 Spectroscopic Study of the Phase Transition of Amorphous to Crystalline  $\beta$ -Carbonic Acid.  
339 *Angewandte Chemie International Edition*, 48, 2690-2694.

340

341 Lam, R.K., England, A.H., Sheardy, A.T., Shih, O., Smith, J.W., Rizzuto, A.M., Prendergast, D.,  
342 and Saykally, R.J. (2014) The hydration structure of aqueous carbonic acid from X-ray  
343 absorption spectroscopy. *Chemical Physics Letters*, 614, 282-286.

344

345 Loerting, T., Tautermann, C., Kroemer, R.T., Kohl, I., Hallbrucker, A., Mayer, E., and Liedl,  
346 K.R. (2000) On the Surprising Kinetic Stability of Carbonic Acid (H<sub>2</sub>CO<sub>3</sub>). *Angewandte*  
347 *Chemie International Edition*, 39, 891-894.

348

349 Massani, B., Mitterdorfer, C., and Loerting, T. (2017) Formation and decomposition of CO<sub>2</sub>-  
350 filled ice. *The Journal of Chemical Physics*, 147, 134503.



351

352 Mitterdorfer, C., Bernard, J., Klauser, F. Winkel, K., Kohl, I., Liedl, K.R., Grothe, H., Mayer, E.,  
353 and Loerting, T. (2012) Local structural order in carbonic acid polymorphs: Raman and FT-  
354 IR spectroscopy. *Journal of Raman Spectroscopy*, 43, 108-115.

355

356 Moore, M.H., and Khanna, R.K. (1991) Infrared and mass spectral studies of proton irradiated  
357 H<sub>2</sub>O + CO<sub>2</sub> ice: evidence for carbonic acid. *Spectrochimica Acta*, 47A, 255-262.

358

359 Mori, T., Suma, K., Sumiyoshi, Y., and Endo, Y. (2009) Spectroscopic detection of isolated  
360 carbonic acid. *The Journal of Chemical Physics*, 130, 204308.

361

362 Mori, T., Suma, K., Sumiyoshi, Y., and Endo, Y. (2011) Spectroscopic detection of the most  
363 stable carbonic acid, *cis-cis* H<sub>2</sub>CO<sub>3</sub>. *The Journal of Chemical Physics*, 134, 044319.

364

365 Oba, Y., Watanabe, N., Kouchi, A., Hama, T., and Pirronello, V. (2010) Formation of carbonic  
366 acid (H<sub>2</sub>CO<sub>3</sub>) by surface reactions of non-energetic OH radicals with CO molecules at low  
367 temperatures. *The Astrophysical Journal*, 722, 1598-1606.

368

369 Oxford Diffraction (2006) ABSPACK (ver. 1.171.32.3), Oxford Diffraction Ltd, Abingdon,  
370 Oxfordshire, England.

371

- 372 Reddy, S.K., Kulkarni, C.H., and Balasubramanian, S. (2011) Theoretical investigations of  
373 candidate crystal structures for  $\beta$ -carbonic acid. The Journal of Chemical Physics, 134,  
374 124511.  
375
- 376 Reisenauer, H.P., Wagner, J.P., and Schreiner, P.R. (2014) Gas-Phase Preparation of Carbonic  
377 Acid and Its Monomethyl Ester. Angewandte Chemie International Edition, 53, 11766-  
378 11771.  
379
- 380 Rigaku Oxford Diffraction (2015) CrysAlisPro (ver. 1.171.38.43), Yarnton, England.  
381
- 382 Saleh, G., and Oganov, A.R. (2016) Novel Stable Compounds in the C-H-O Ternary System at  
383 High Pressure. Scientific Reports, 6, 32486.  
384
- 385 Sheldrick, G.M. (2015) Crystal structure refinement with *SHELXL*. Acta Crystallographica C,  
386 71, 3-8.  
387
- 388 Sloan, E.D. Jr., and Koh, C. (2007) Clathrate Hydrates of Natural Gases, Third Edition, 752 p.  
389 CRC Press, Boca Raton.  
390
- 391 Soli, A.L., and Byrne, R.H. (2002) CO<sub>2</sub> system hydration and dehydration kinetics and the  
392 equilibrium CO<sub>2</sub>/H<sub>2</sub>CO<sub>3</sub> ratio in aqueous NaCl solution. Marine Chemistry, 78, 65-73.  
393

- 394 Terlouw, J.K., Lebrilla, C.B., and Schwarz, H. (1987) Thermolysis of  $\text{NH}_4\text{HCO}_3$  – A Simple  
395 Route to the Formation of Free Carbonic Acid ( $\text{H}_2\text{CO}_3$ ) in the Gas Phase. *Angewandte*  
396 *Chemie International Edition*, 26, 354-355.
- 397
- 398 Tulk, C.A., Machida, S., Klug, D.D., Lu, H., Guthrie, M., and Molaison, J.J. (2014) The  
399 structure of  $\text{CO}_2$  hydrate between 0.7 and 1.0 GPa. *The Journal of Chemical Physics*, 141,  
400 174503.
- 401
- 402 Wang, H., Zeuschner, J., Eremets, M., Troyan, I., and Williams, J. (2016) Stable solid and  
403 aqueous  $\text{H}_2\text{CO}_3$  from  $\text{CO}_2$  and  $\text{H}_2\text{O}$  at high pressure and high temperature. *Scientific Reports*,  
404 6, 19902.
- 405
- 406 Waasmaier, D., and Kirfel, A. (1995) New analytical scattering-factor functions for free atoms  
407 and ions. *Acta Crystallographica A*, 51, 416-431.
- 408
- 409 Winkel, K., Hage, W., Loerting, T., Price, S.L., and Mayer, E. (2007) Carbonic Acid: From  
410 Polyamorphism to Polymorphism. *Journal of the American Chemical Society*, 129, 13863-  
411 13871.
- 412
- 413 Wu, C.Y.R., Judge, D.L., Cheng, B.-M., Yih, T.-S., Lee, C.S., and Ip, W.H. (2003) Extreme  
414 ultraviolet photolysis of  $\text{CO}_2$  -  $\text{H}_2\text{O}$  mixed ices at 10 K. *Journal of Geophysical Research:*  
415 *Planets*, 108, 5032.

416

417 Zeller, K.-P., Schuler, P., and Haiss, P. (2005) The Hidden Equilibrium in Aqueous Sodium  
418 Carbonate Solutions – Evidence for the Formation of the Dicarbonate Anion. European  
419 Journal of Inorganic Chemistry, 2005, 168-172.

420

421 Zhang, L., Huang, X., Qin, C., Brinkman, K., Gong, Y., Wang, S., and Huang, K. (2013) First  
422 spectroscopic identification of pyrocarbonate for high CO<sub>2</sub> flux membranes containing highly  
423 interconnected three dimensional ionic channels. Physical Chemistry Chemical Physics, 15,  
424 13147-13152.

425

426 Zheng, W., and Kaiser, R.I. (2007) On the formation of carbonic acid (H<sub>2</sub>CO<sub>3</sub>) in solar system  
427 ices. Chemical Physics Letters, 450, 55-60.

428

429 **Figure Captions**

430

431 Figure 1. **(a)** Photomicrograph of the pressure chamber during growth of euhedral crystals from  
432 the fluid phase. **(b)** After cooling to room temperature. The small, dark cross-hairs indicate the  
433 approximate location of X-ray impingement during data collection.

434 Figure 2. ORTEP of the structure with thermal ellipsoids at the 50% probability level.

435 Figure 3. **(a)** Illustration of the layered structure of the crystal with the (110) sheets. The box of  
436 solid, black lines represents the unit cell dimensions. **(b)** View perpendicular to a (110) sheet,  
437 showing the cis-trans configuration of the carbonic acid molecules and hydrogen-bonded chains  
438 of H<sub>2</sub>CO<sub>3</sub> along the c-axis. C, O and H atoms are depicted as black, red and pink spheres,  
439 respectively.

440

# Figure 1

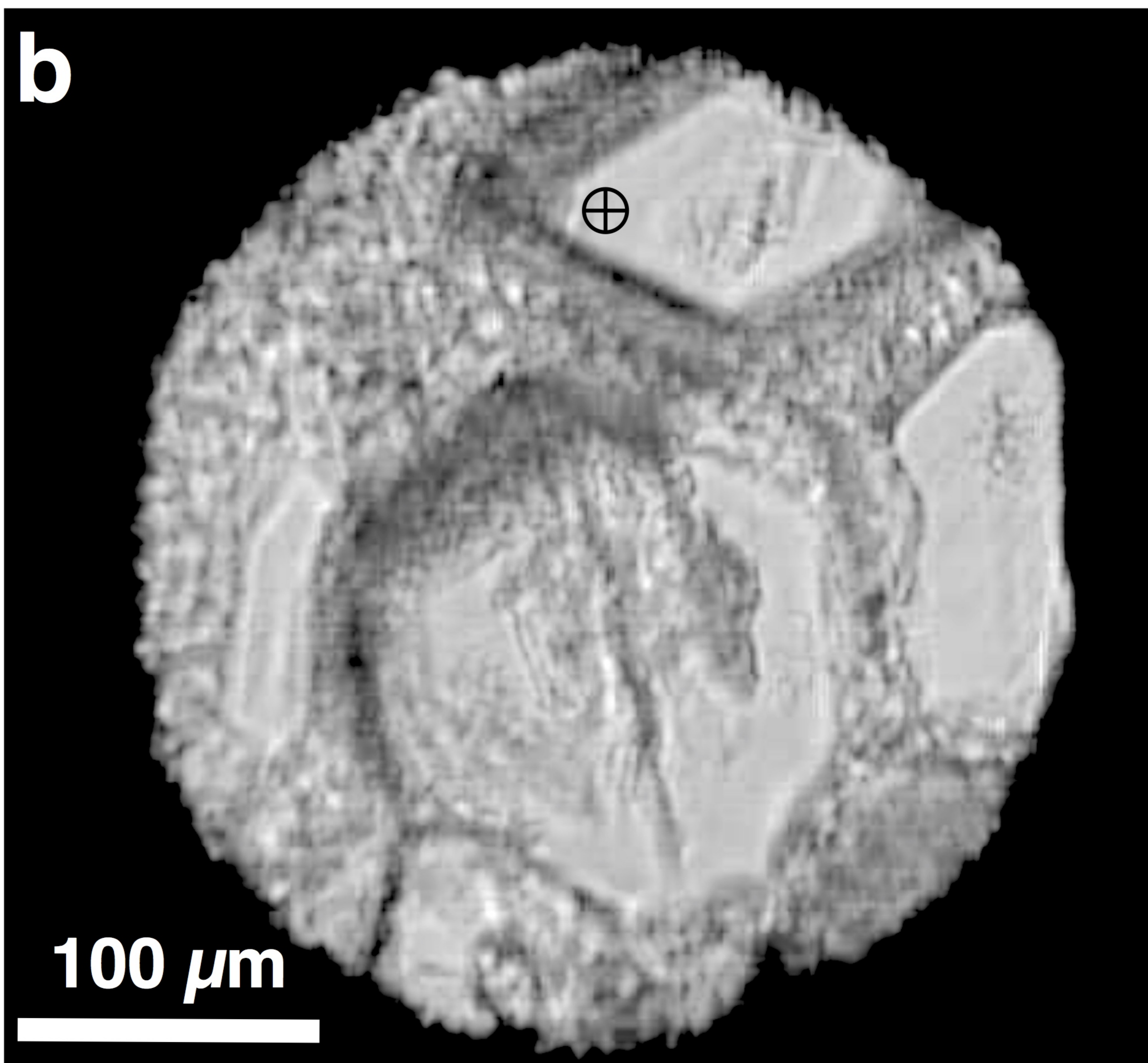
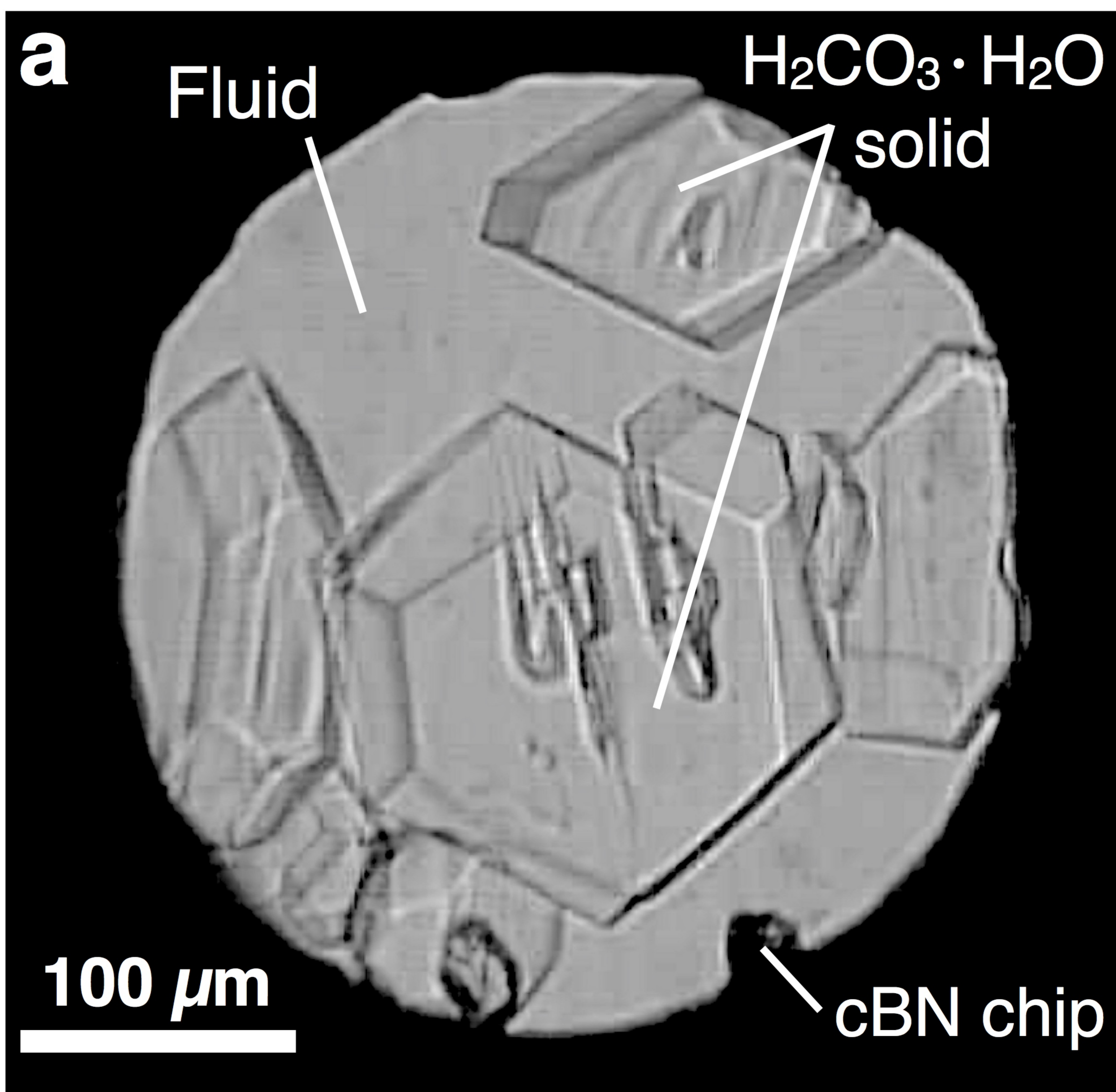


**Figure 2**

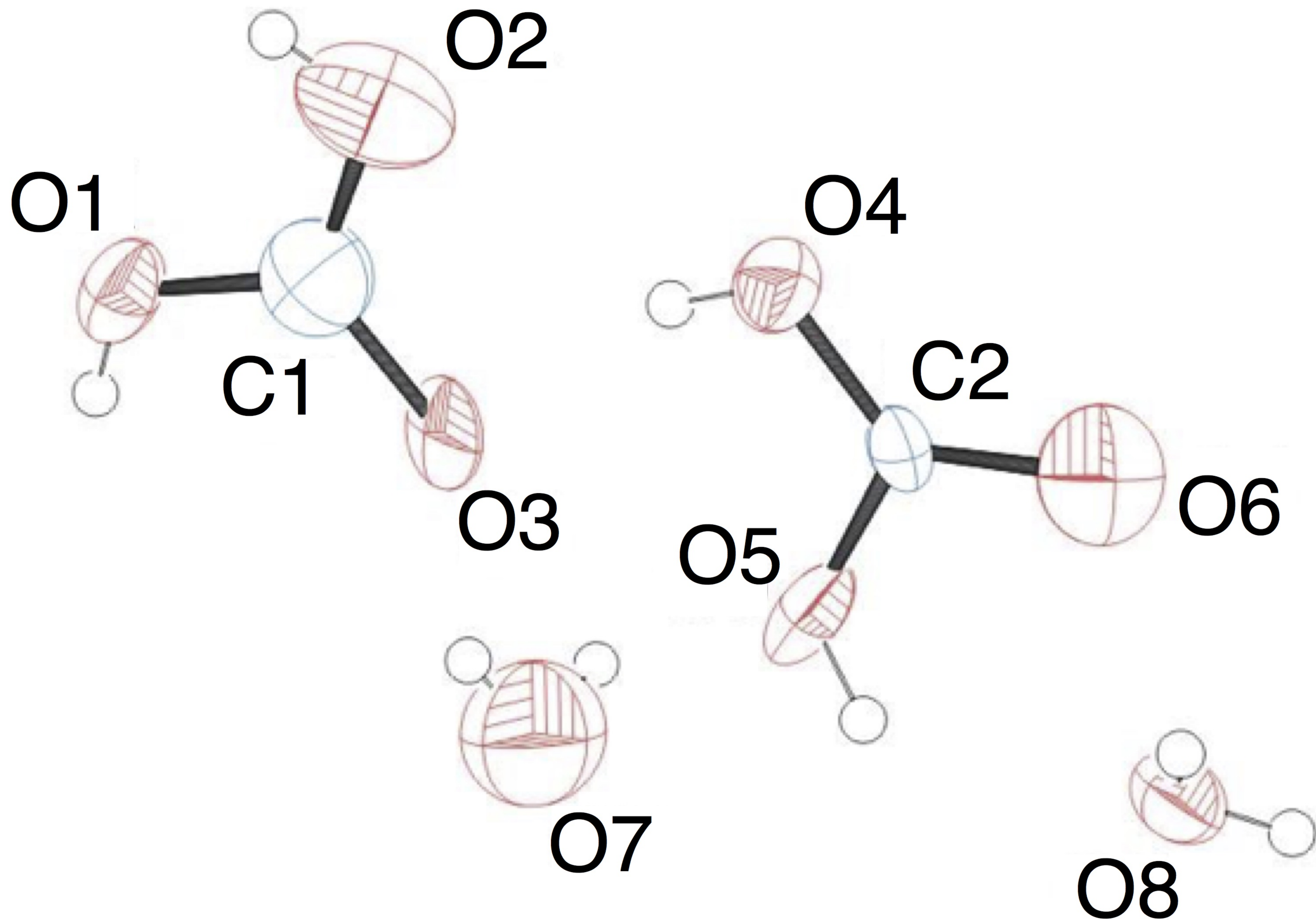


**Figure 3**

